Inorg. Chem. **2006**, *45*, 849–857

Metal–Metal Interactions in Thallium(I)/Platinum(II) Compounds Involving a Chelating Dicarbene and Various Auxiliary Ligands

Jay R. Stork, Marilyn M. Olmstead, James C. Fettinger, and Alan L. Balch*

Department of Chemistry, University of California, Davis, California 95616

Received July 26, 2005

Reaction of $Tl^{I}NO_3$ and $(C_4H_{10}N_4)Pt^{II}$(mnt) or $(C_4H_{10}N_4)Pt^{II}$(dmg-H) [mnt = maleonitriledithiolate, dmg-H = dimethylglyoximate dianion] in dilute, aqueous KOH yielded adducts of Tl^{I} and the conjugate bases of the platinum(II) compounds. The compound $Tl^{I}[(C_4H_9N_4)Pt^{II}(dmg\text{-}H)]\cdot 5H_2O$ forms as dimers with close $Tl^{I}\cdots Pt^{II}$ separations of 3.0843(5) Å, while $Tl^{I}[(C_4H_9N_4)Pt^{II}(mnt)]$ has much longer $Tl^{I}\cdots Pt^{II}$ separations of 3.4400(2) Å and forms loosely associated, helical coordination polymers. The new compounds are compared with the red and yellow polymorphs of $Tl^{I}[(C_4H_9N_4)Pt^{II}(CN)_2]$, and the influences of crystal packing forces, Coulombic interactions, and hydrogen bonding on supramolecular structures and $Tl^{I}\cdots Pt^{II}$ separations are discussed.

Introduction

Metal ions with d^8, d^{10}, and s^2 electronic configurations, particularly Pt(II), Au(I), and Tl(I), are well known to interact with one another to form weak metal−metal bonds.[1] These bonds form important features of the structures of these compounds. However, because such closed-shell and pseudo-closed-shell interactions tend to be rather weak, the supramolecular architectures formed thereby often can be perturbed by variations in other weak interactions such as hydrogen-bonding, counterion charge and size, or crystal field effects. For example, in the well-studied tetracyanoplatinate(II) salts, the anions associate through d^8-d^8, interactions with a variety of Pt···Pt separations that depend on the cation and water of crystallization.[2] We have also shown that the $Pt^{II}\cdots Pt^{II}$ interactions in salts of Chugaev's cation, $[(C_4H_9N_4)Pt^{II}(CNCH_3)_2]^+$ (for structure, see Scheme 1), vary with differences in anion and solvent of crystallization.[3] In these salts, the cations associate through a variety of motifs including staggered, zigzag chains of platinum atoms, helical chains with more nearly uniform $Pt^{II}\cdots Pt^{II}$ separations, hydrogen-bonded tetramers with close $Pt^{II}\cdots Pt^{II}$ contacts, and loosely associated dimers. Neutral gold(I) isocyanide compounds, $(RNC)Au^{I}X$, (X = Cl, Br, I, CN) associate through aurophilic, $Au^{I}\cdots Au^{I}$ ($d^{10}-d^{10}$) interactions having various separations with different choices of X and R group.[4] Heterometallic d^8-d^{10} and d^8-s^2 interactions are somewhat less well known.[5−11] The present paper concerns heterometallic interactions of the d^8-s^2 variety.

Metallophilic interactions can be abetted by ionic bonding, particularly when the metals are incorporated as oppositely charged complexes. This Coulombic attraction is seen in such compounds as the $[Pt^{II}(CNR)_4][Pt^{II}(CN)_4]$ double salts[12,13] and $Tl^{I}_2[Pt^{II}(CN)_4]$.[5−7] We recently reported the synthesis of

(1) (a) Pyykkö, P. *Chem. Rev.* **1997**, *97*, 597. (b) Pyykkö, P. *Angew. Chem., Int. Ed.* **2004**, *43*, 4412.
(2) Williams, J. M.; Schultz, A. J.; Underhill, A. E.; Carneiro, K. In *Extended Linear Chain Comounds;* Miller, J. S., Ed.; Plenum: New York, 1982; vol. 1, p 73.
(3) Stork, J. R.; Olmstead, M. M.; Balch, A. L. *Inorg. Chem.* **2004**, *43*, 7508.
(4) (a) Bachman, R. E.; Fioritto, M. S.; Fetics, S. K.; Cocker, T. M. *J. Am. Chem. Soc.* **2001**, *123*, 5376. (b) Ecken, H.; Olmstead, M. M.; Noll, B. C.; Attar, S.; Schlyer, B.; Balch, A. L. *J. Chem. Soc., Dalton Trans.* **1998**, 3715. (c) Liau, R.-Y.; Mathieson, T.; Schier, A.; Berger, R. J. F.; Runeberg, N.; Schmidbaur, H. *Z. Naturforsch., B: Chem. Sci.* **2002**, *57*, 881. (d) Siemeling, U.; Rother, D.; Bruhn, C.; Fink, H.; Weidner, T.; Traeger, F.; Rothenberger, A.; Fenske, D.; Priebe, A.; Maurer, J.; Winter, R. *J. Am. Chem. Soc.* **2005**, *127*, 1102. (e) White-Morris, R. L.; Olmstead, M. M.; Balch, A. L.; Elbjeirami, O.; Omary, M. A. *Inorg. Chem.* **2003**, *42*, 6741. (f) Elbjeirami, O., Omary, M. A., Stender, M., Balch, A. L. *Dalton Trans*. **2004**, 3173. (g) White-Morris, R. L., Stender, M., Tinti, D. S., Balch, A. L. *Inorg. Chem*. **2003**, *42*, 3237.
(5) Nagle, J. K.; Balch, A. L.; Olmstead, M. M. *J. Am. Chem. Soc.* **1988**, *110*, 319.
(6) Nagle, J. K.; Lacasce, J. H., Jr.; Dolan, P. J., Jr.; Corson, M. R.; Assefa, Z.; Patterson, H. H. *Mol. Cryst. Liq. Cryst.* **1990**, *181*, 359.
(7) Ziegler, T.; Nagle, J. K.; Snijders, J. G.; Baerends, E. J. *J. Am. Chem. Soc.* **1989**, *111*, 5631.
(8) Bennett M. A.; Contel, M.; Hockless, D. C. R.; Welling L. L.; Willis, A. C. *Inorg. Chem.* **2002**, *41*, 844.
(9) Dolg, M.; Pyykkö, P.; Runeberg, N. *Inorg. Chem.* **1996**, *35*, 7450.
(10) Xia, B.-H.; Zhang, H.-X.; Jiao, Y.-Q.; Pan, Q.-J.; Li, Z.-S.; Sun, C.-C. *J. Chem. Phys.* **2004**, *120*, 11487.
(11) Stork, J. R.; Rios, D.; Pham, D.; Bicocca, V.; Olmstead, M. M.; Balch, A. L. *Inorg. Chem.* **2005**, *44*, 3466.
(12) Buss, C. E.; Anderson, C. E.; Pomije, M. K.; Lutz, C. M.; Britton, D.; Mann, K. R. *J. Am. Chem. Soc.* **1998**, *120*, 7783.
(13) Isci, H.; Mason, W. R. *Inorg. Chem.* **1974**, *13*, 1175.

10.1021/ic051252+ CCC: $33.50
Published on Web 12/16/2005

Scheme 1

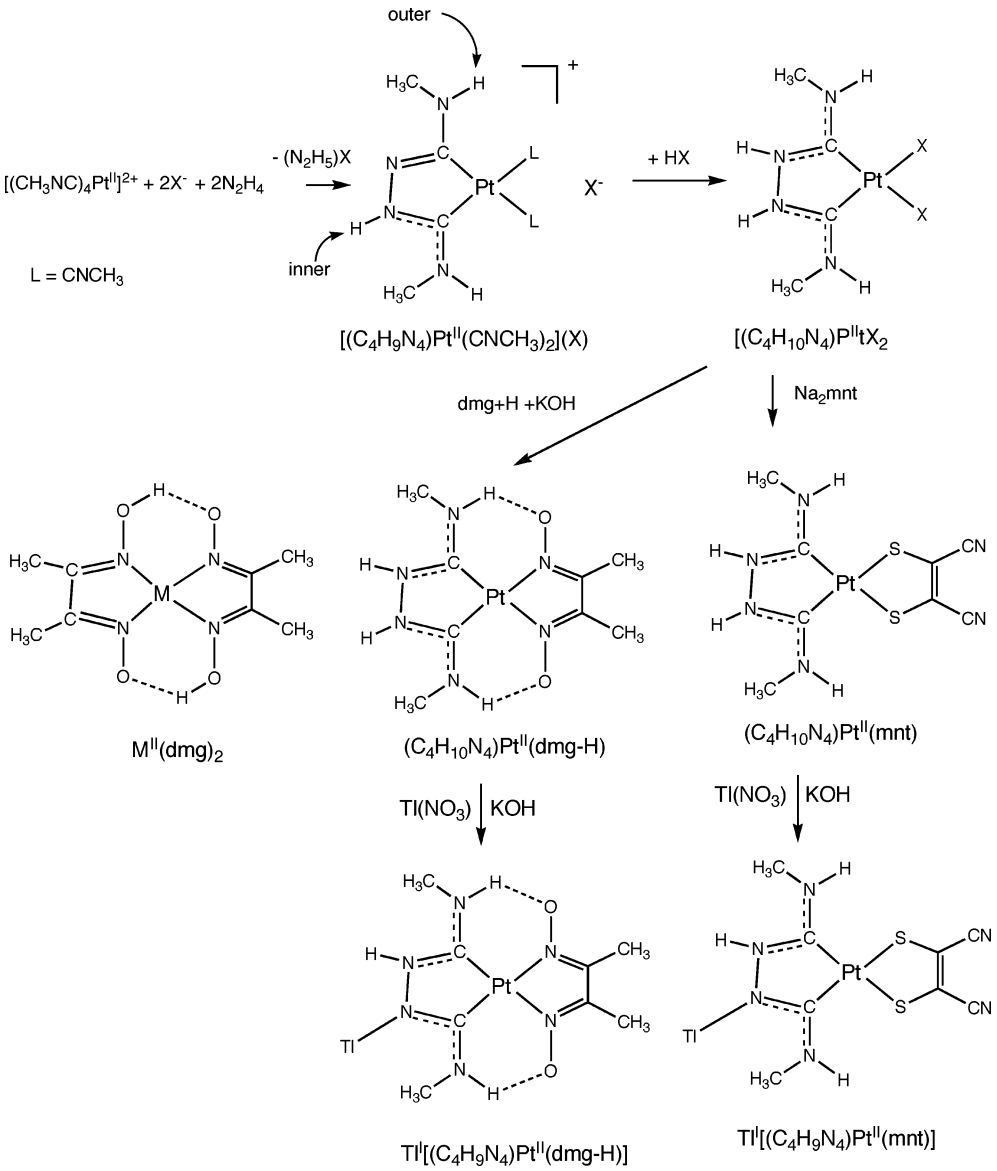

polymorphic organometallic coordination polymers derived from the addition of Tl^{I} to the anion $[(C_4H_9N_4)Pt^{II}(CN)_2]^-$.[14] In that work, we found that the color of the crystalline solid was related to differences in the extent of $Tl^{I}\cdots Pt^{II}$ interactions, with a red form of $Tl^{I}[(C_4H_9N_4)Pt^{II}(CN)_2]$ that has an extended chain of $Pt^{II}\cdots(Tl^{I}\cdots Pt^{II})_n\cdots Tl^{I}$ contacts and a yellow form that lacks the extended bonding but forms dimers with $Tl^{I}\cdots Pt^{II}$ interactions. Inspired by our success, we set out to see whether related anionic Pt^{II} complexes, in which the cyano groups were replaced by other ligands, might have similar affinity toward Tl^{I} and how the variation in auxiliary ligands might affect the $Tl^{I}\cdots Pt^{II}$ interactions. In the current report, we discuss the synthesis and crystallographic characterization of two new compounds with $Tl^{I}\cdots Pt^{II}$ interactions, $Tl^{I}[(C_4H_9N_4)Pt^{II}(mnt)]$ and $Tl^{I}[(C_4H_9N_4)Pt^{II}(dmg\text{-}H)]\cdot 5H_2O$ (where mnt = maleonitriledithiolate and dmg-H = dimethylglyoximate dianion), and provide a more complete crystallographic characterization of the hydrogen bonding in these and in the red and yellow polymorphs of $Tl^{I}[(C_4H_9N_4)Pt^{II}(CN)_2]$.

Results

The synthetic work involved in this project is summarized in Scheme 1. Pale yellow $(C_4H_{10}N_4)Pt^{II}Cl_2$ was prepared from $[Pt^{II}(CNCH_3)_4]^{2+}$ as described previously.[15,16] Treatment of $(C_4H_{10}N_4)Pt^{II}Cl_2$ with dimethylglyoxime (dmg+H) in basic solution produces yellow $(C_4H_{10}N_4)Pt^{II}$(dmg-H).[17] Treatment of this complex with potassium hydroxide and thallium(I) nitrate produces brick red $Tl^{I}[(C_4H_9N_4)Pt^{II}(dmg\text{-}H)]$. Similarly, addition of sodium maleonitrile dithiolate (Na_2mnt) to a solution of $(C_4H_{10}N_4)Pt^{II}Cl_2$ in aqueous ammonia produces $(C_4H_{10}N_4)Pt^{II}$(mnt). Addition of potassium hydroxide and

(14) Stork, J. R.; Olmstead, M. M.; Balch, A. L. *J. Am. Chem. Soc.* **2005**, *127*, 6512.

(15) Burke, A.; Balch, A. L.; Enemark, J. H. *J. Am. Chem. Soc.* **1970**, *92*, 2555.

(16) Butler, W. M.; Enemark, J. H.; Parks, J.; Balch, A. L. *Inorg. Chem.* **1973** *12*, 451.

(17) Rouschias, G.; Shaw, B. L. *J. Chem. Soc. (A)* **1971**, 2097.

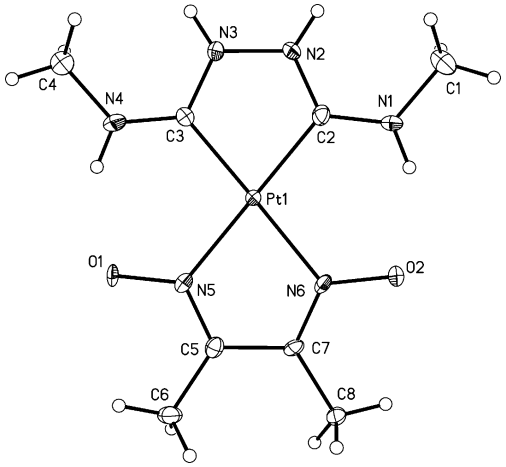

Figure 1. A drawing showing the molecular structure of $[(C_4H_{10}N_4)Pt^{II}$-(dmg-H)]·$3H_2O$ with 50% thermal contours. Selected distances (Å). Molecule 1: Pt1−C3, 1.964(6); Pt1−C2, 1.980(7); Pt1−N5, 2.041(5); Pt1−N6, 2.053(4); C1−N1, 1.474(8); C2−N2, 1.307(9); C2−N1, 1.321(9); C3−N4, 1.306(10); C3−N3, 1.345(10); C4−N4, 1.470(9); N2−N3, 1.406(9); N5−O1, 1.332(7); N6−O2, 1.357(7); O1···N4, 2.832(8); O2···N1, 2.834-(9). Molecule 2: Pt2−C11, 1.975(6); Pt2−C10, 1.983(6); Pt2−N11, 2.046-(4); Pt2−N12, 2.049(4) C(9)−N(7) 1.445(9); C10−N7, 1.334(9); C10−N8, 1.335(11); C11−N10, 1.323(9); C11−N9, 1.366(9); C12−N10, 1.433(7); C13−N11, 1.310(8); N8−N9, 1.414(9); O3···N10, 2.798(9); O4···N7, 2.861(8). Selected angles (deg). Molecule 1: C3−Pt1−C2, 79.4(3); C3−Pt1−N5, 100.6(3); C2−Pt1−N5, 179.03(18); C3−Pt1−N6, 178.9(2); C2−Pt1−N6, 101.6(3); N5−Pt1−N6, 78.3(2). Molecule 2: C11−Pt2−C10, 80.0(3); C11−Pt2−N11, 99.9(3); C10−Pt2−N11, 178.86(14); C11−Pt2−N12, 178.2(3); C10−Pt2−N12, 101.6(3); N11−Pt2−N12, 78.5(2).

thallium(I) nitrate to pink $(C_4H_{10}N_4)Pt^{II}$(mnt) produces orange-tan $Tl^I[(C_4H_9N_4)Pt^{II}$(mnt)]. Each of these four complexes has been characterized by X-ray crystallography as outlined in the following sections.

Crystallographic Structures of $(C_4H_{10}N_4)Pt^{II}$(dmg-H)·$3H_2O$ and $Tl^I[(C_4H_9N_4)Pt^{II}$(dmg-H)]·$5H_2O$. Yellow needles of $[(C_4H_{10}N_4)Pt^{II}$(dmg-H)]·$3H_2O$ crystallize with two molecules of the platinum complex in the asymmetric unit. Neither molecule has any crystallographically imposed symmetry. Figure 1 shows a drawing of Molecule 1. Molecule 2 is similar. Selected bond distances and angles for both nearly planar molecules are given in the figure caption. $[(C_4H_{10}N_4)Pt^{II}$(dmg-H)]·$3H_2O$ differs from the traditional $M^{II}(dmg)_2$ complexes in that the (dmg-H) dianion is present in the former while the (dmg) anion is present in the latter. Previous work has demonstrated that complexes containing the dmg monoanion can be deprotonated.[18] In $[(C_4H_{10}N_4)Pt^{II}$(dmg-H)]·$3H_2O$, each oxygen atom of the dmg-H dianion acts as a hydrogen-bond acceptor with the outer N−H protons of the chelating dicarbene ligand acting as the H-bond donors. This arrangement produces a pseudo-macrocyclic structure that is reminiscent of that found in classic $M^{II}(dmg)_2$ complexes as shown in Scheme 1. There are no close Pt···Pt contacts in $[(C_4H_{10}N_4)Pt^{II}$(dmg-H)]·$3H_2O$. The shortest intermolecular Pt···Pt distance is 6.8755(7) Å.

Brick red $Tl^I[(C_4H_9N_4)Pt^{II}$(dmg-H)]·$5H_2O$ crystallizes with one $Tl^I[(C_4H_9N_4)Pt^{II}$(dmg-H)] unit and five water molecules in the asymmetric unit, all in general positions. A view of the planar $Tl^I[(C_4H_9N_4)Pt^{II}$(dmg-H)] unit is shown in Figure 2. This view shows that the thallium atom is coordinated to an inner imine nitrogen atom of the dicarbene ligand.

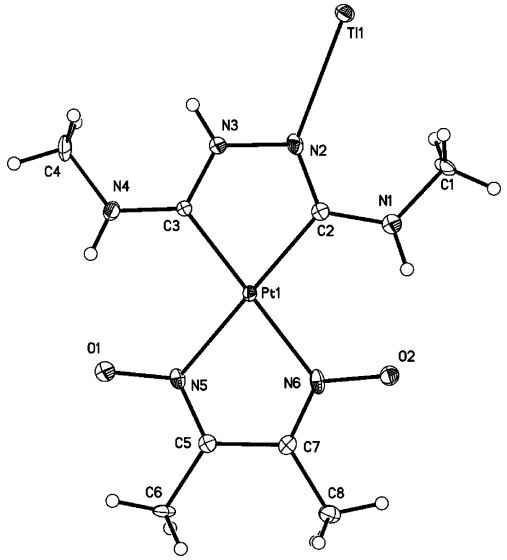

Figure 2. A drawing of the molecular structure of $Tl^I[(C_4H_9N_4)Pt^{II}$-(dmg-H)]·$5H_2O$ with 50% thermal contours. Selected distances (Å): Pt1−C2, 1.993(8); Pt1−C3, 1.976(7); Pt1−N5, 2.058(6); Pt1−N6, 2.048(7); Tl1−N2, 2.578(6); C1−N1, 1.449(9); C2−N2, 1.330(9); C2−N1, 1.335-(9); C3−N3, 1.312(9); C3−N4, 1.340(9); C4−N4, 1.445(10); C5−N5, 1.321(10); C5−C7, 1.475(10); C7−N6, 1.300(10); N2−N3, 1.424(8); O2···N1, 2.831(9); O1···N4, 2.959(9); N2−Tl1, 2.578(6). Selected angles (deg): C2−Pt1−C3, 78.3(3); C2−Pt1−N6, 101.8(3); C3−Pt1−N5 102.1-(3); N5−Pt1−N6, 77.8(2); C(3)−Pt1-N6, 179.5(3); C2−Pt1−N5, 175.5-(3); N2−Tl1−Pt1A, 88.19(14).

Otherwise, the structure of this unit is similar to that of $[(C_4H_{10}N_4)Pt^{II}$(dmg-H)], which is shown in Figure 1.

In addition to the coordination to an inner imine nitrogen atom of the dicarbene ligand, the thallium ion in Tl^I-$[(C_4H_9N_4)Pt^{II}$(dmg-H)]·$5H_2O$ is also bonded to a water molecule and to a platinum ion of an adjacent complex. The structure of the centrosymmetric dimeric entity that results from the presence of the Tl···Pt bonding is shown in Figure 3. This dimeric unit is very similar to the dimeric unit found in the yellow polymorph of $Tl^I[(C_4H_9N_4)]Pt^{II}(CN)_2]$, as can be seen in part B of Figure 3. While the yellow polymorph of $Tl^I[(C_4H_9N_4)]Pt^{II}(CN)_2]$ has a Tl···Pt separation of 3.0256-(5) Å, the Tl···Pt separation in $Tl^I[(C_4H_9N_4)Pt^{II}$(dmg-H)] is slightly longer, 3.0843(5) Å.

Additionally, the dimers of $Tl^I[(C_4H_9N_4)Pt^{II}$(dmg-H)] are linked via hydrogen bonding of the dimethylglyoximate oxygens to chains of water molecules as seen in Figure 4. These interstitial water molecules form ribbons of $(H_2O)_4$ tetramers with a T4(0)A(0) topology.[19,20]

For comparison with Figure 4, sections through layers within the structures of the red and yellow polymorphs of $Tl^I[(C_4H_9N_4)]Pt^{II}(CN)_2]$ are shown in Figure 5. The red polymorph has a strictly layered structure with ribbons that are connected by hydrogen bonds between the inner N−H group of one complex and a cyano ligand in the adjacent complex and by coordination of the thallium ion by the nitrile group of the neighboring complex. The yellow complex also has a somewhat layered structure, as seen in part B of Figure

(18) Bell-Loncella, E. T.; Bessel, C. A. *Inorg. Chim. Acta* **2000**, *303*, 199.
(19) Infantes, L.; Motherwell, S. *CrystEngComm* **2002**, *4*, 454.
(20) Infantes, L.; Chisholm, J.; Motherwell, S. *Cryst. Eng. Comm.* **2003**, *5*, 480.

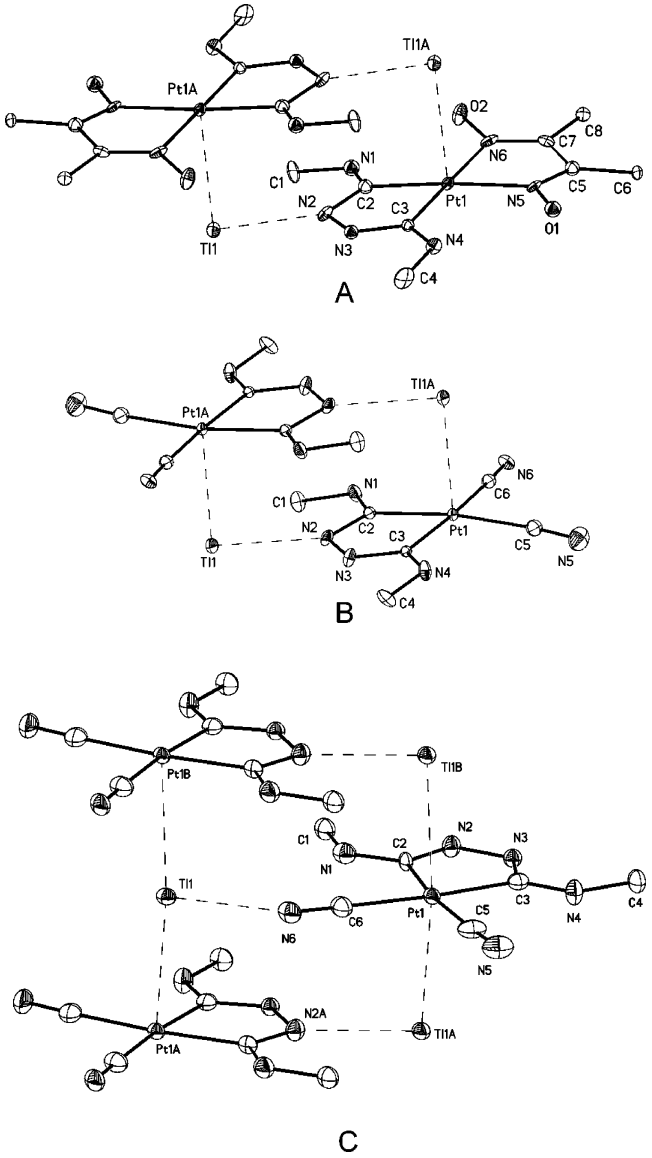

Figure 3. (A) A drawing of the centrosymmetric dimer in $Tl^{I}[(C_4H_9N_4)Pt^{II}(dmg\text{-}H)]\cdot 5H_2O$ with 50% thermal contours. The Tl···Pt distance is 3.0843(5) Å, and the N2−Tl1−Pt1A angle is 88.19(14). (B) A drawing of the centrosymmetric dimer in the yellow polymorph of $Tl^{I}[(C_4H_9N_4)Pt^{II}(CN)_2]$ with 50% thermal contours. The Tl···Pt distance is 3.0256(5) Å. (C) A drawing of the red polymorph of $Tl^{I}[(C_4H_9N_4)Pt^{II}(CN)_2]$ with 50% thermal contours. The Tl···Pt distance is 3.0978(2) Å.

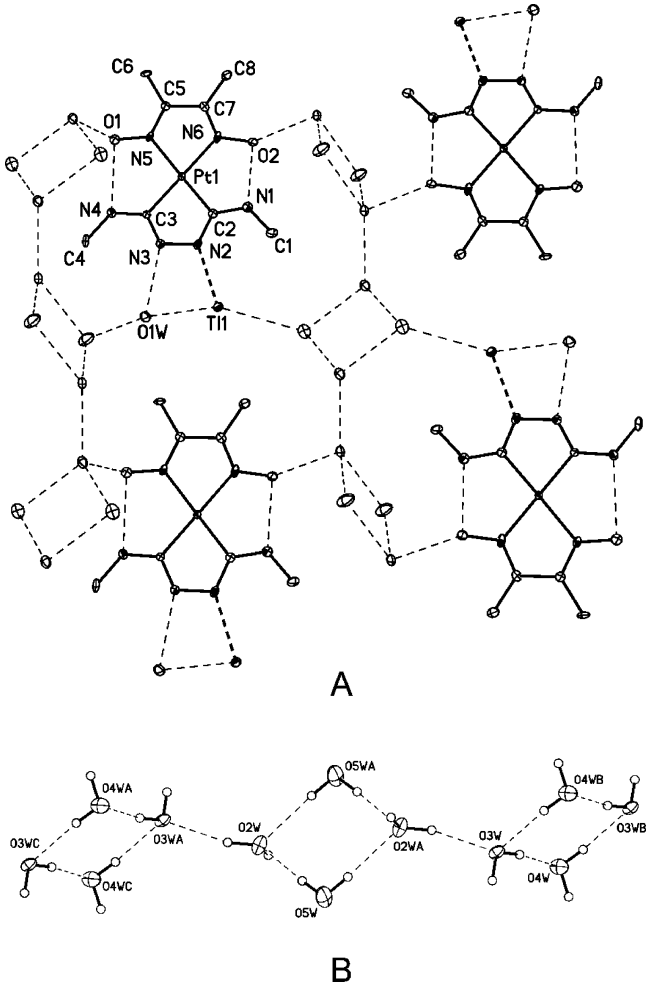

Figure 4. (A) A drawing of a portion of the hydrogen-bonding network in $Tl^{I}[(C_4H_9N_4)Pt^{II}(dmg\text{-}H)]\cdot 5H_2O$ with 50% thermal contours for all non-hydrogen atoms. (B) Detail of the ribbon of water molecules in $Tl^{I}[(C_4H_9N_4)Pt^{II}(dmg\text{-}H)]\cdot 5H_2O$.

5. Here the outer six complexes lie in a plane, but the inner three complexes are twisted out of that plane by a glide plane operation.

Crystallographic Structures of $(C_4H_{10}N_4)Pt^{II}(mnt)\cdot H_2O$ and $Tl^{I}[(C_4H_9N_4)Pt^{II}(mnt)]$. Crystals of $(C_4H_{10}N_4)Pt^{II}(mnt)\cdot H_2O$ contain one complex molecule and one water molecule in general positions in the asymmetric unit. Figure 6 shows a drawing of the nearly planar platinum complex. All of the bond distances in this complex fall in normal ranges. As is the case with $[(C_4H_{10}N_4)Pt^{II}(dmg\text{-}H)]\cdot 3H_2O$, there are no unusually close $Pt^{II}\cdots Pt^{II}$ interactions between these complexes. The shortest intermolecular $Pt^{II}\cdots Pt^{II}$ separation is 4.8466(6) Å.

The asymmetric unit of $Tl^{I}[(C_4H_9N_4)Pt^{II}(mnt)]$ contains a single molecular unit with all atoms in general positions. Figure 7 show a drawing of this planar unit. Again, the thallium ion is bonded to one of the inner imine nitrogen atoms of the chelating carbene ligand. In crystalline $Tl^{I}[(C_4H_9N_4)Pt^{II}(mnt)]$, the constituent ions are arranged into a helical, one-dimensional coordination polymer that is generated by a 2_1 screw axis. A portion of this helical chain is shown in Figure 8. In this polymer, the anions are connected by Tl^{I}−N(imine) bonds and close $Tl^{I}\cdots Pt^{II}$ contacts. The $Pt^{II}\cdots Tl^{I}$−N angle is 102.59(6) °. The Tl^{I}−N separation of 2.708(3) Å is slightly longer than in the $Tl^{I}[(C_4H_9N_4)Pt^{II}(CN)_2]$ compounds. At 3.4400(2) Å, the $Tl^{I}\cdots Pt^{II}$ separation is somewhat less than the sum of the van der Waals radii, but it is significantly greater than in the previous structures. A search of the CSD found this to be by far the longest Tl^{I}−Pt^{II} bond in the database. In $Tl^{I}[(C_4H_9N_4)Pt^{II}(dmg\text{-}H)]$ and the two polymorphs of $Tl^{I}[(C_4H_9N_4)Pt^{II}(CN)_2]$, the planar platinum complexes are all aligned into parallel layers. However, in $Tl^{I}[(C_4H_9N_4)Pt^{II}(mnt)]$, such layering, which facilitates the formation of dimeric entities with two $Tl^{I}\cdots Pt^{II}$ interactions, is absent and the planes of adjacent platinum complexes are tilted as seen in Figure 8. This allows helical ribbons rather than dimers to form.

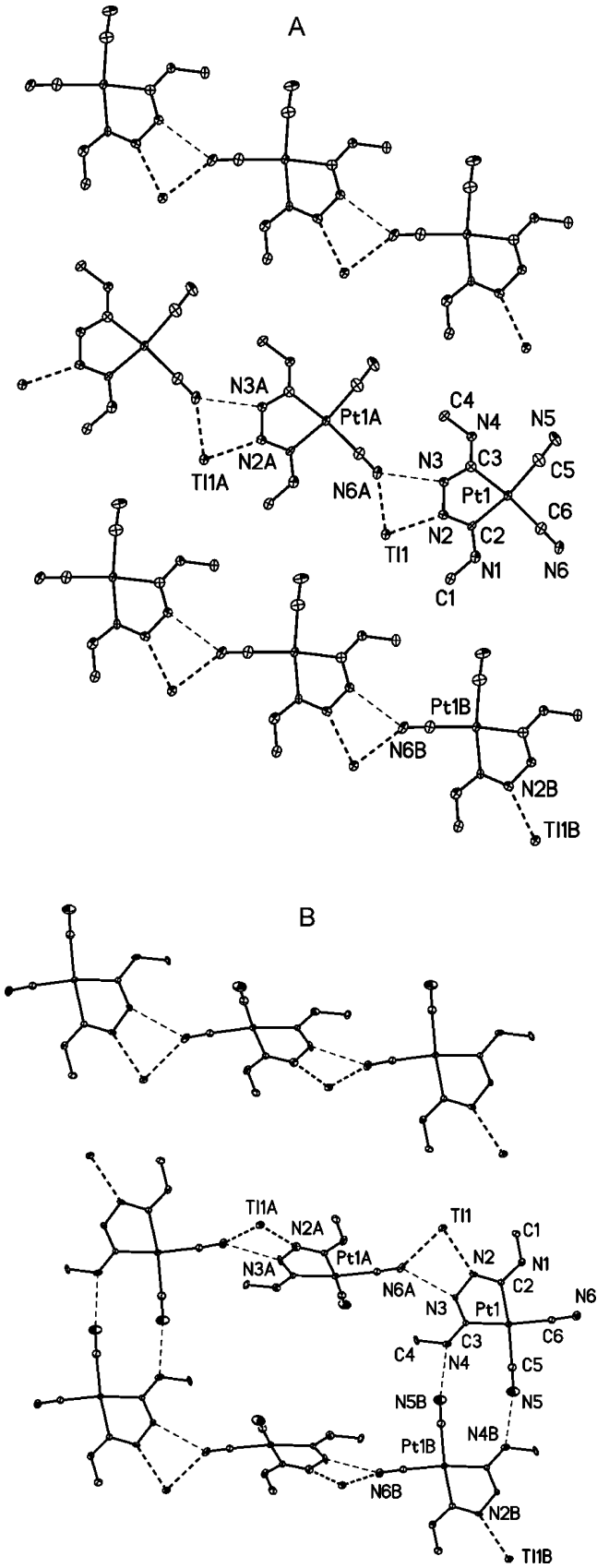

Figure 5. (A) A drawing of a layer within the structure of the red polymorph of $Tl^{I}[(C_4H_9N_4)Pt^{II}(CN)_2]$. The Tl1−N6A distance is 2.691(9) Å, and the N3−N6A distance is 2.894(11) Å. (B) A drawing of a layer (defined by the three molecules on the left and the three molecules on right sides) within the structure of the yellow polymorph of $Tl^{I}[(C_4H_9N_4)Pt^{II}(CN)_2]$. The Tl1−N6A distance is 2.687(7) Å, and the N3−N6A distance is 2.879(9) Å.

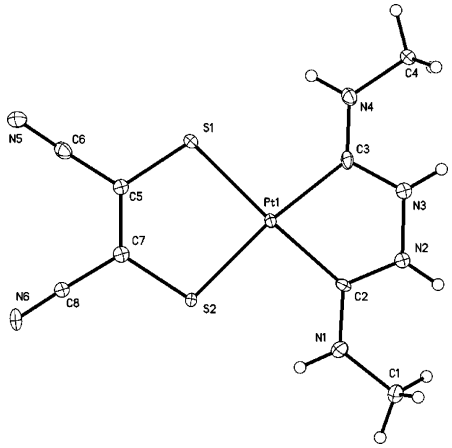

Figure 6. A drawing showing the molecular structure of $(C_4H_{10}N_4)Pt^{II}(mnt)\cdot H_2O$ with 50% thermal contours. Selected distances (Å): Pt1−C2, 1.974(7); Pt1−C3, 1.979(7); Pt1−S1, 2.281(3); Pt1−S2, 2.278(3); C1−N1, 1.450(9); C2−N2, 1.299(16); C2−N1, 1.309(9); C3−N4, 1.286(15); C3−N3, 1.308(8); C4−N4, 1.436(14); C5−C7, 1.362(17); C5−C6, 1.405(11); C5−S1, 1.717(8); C6−N5, 1.147(9); C7−C8, 1.421(9); C7−S2, 1.706(13); C8−N6, 1.122(9); N2−N3, 1.414(15). Selected angles (deg): C2−Pt1−C3, 79.9(3); C2−Pt1−S2, 93.7(2); C3−Pt1−S2, 172.9(3); C2−Pt1−S1, 176.5(2); C3−Pt1−S1, 96.8(2); S2−Pt1−S1, 89.68(7).

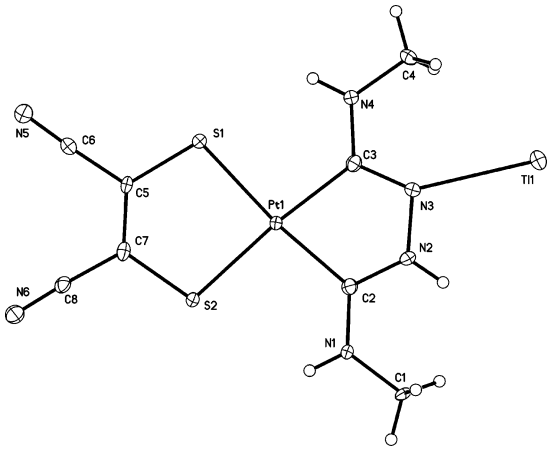

Figure 7. A drawing showing the molecular structure of $Tl^{I}[(C_4H_9N_4)Pt^{II}(mnt)]$ with 50% thermal contours. Selected distances (Å): Pt1−C2, 1.993(3); Tl1−N3, 2.708(3); Pt1−C3, 2.011(3); Pt1−S1, 2.3089(8); Pt1−S2, 2.3212(8); C1−N1, 1.460(4); C2−N2, 1.331(4); C2−N1, 1.339(4); C3−N3, 1.322(4); C3−N4, 1.353(4); C4−N4, 1.444(4); C5−C7, 1.371(4); C5−C6, 1.435(4); C5−S1, 1.740(3); C6−N5, 1.144(4); C7−C8, 1.424(4); C7−S2, 1.738(3); C8−N6, 1.163(4); N2−N3, 1.404(4). Selected angles (deg): Pt1−Tl1−N3, 102.59(6); C2−Pt1−C3, 78.21(13); C2−Pt1−S1, 172.46(10); C3−Pt1−S1, 95.56(9); C2−Pt1−S2, 96.66(10); C3−Pt1−S2, 174.87(9); S1−Pt1−S2, 89.54(3).

Figure 9 shows a stereoscopic view of the coordination environment of the thallium ion in $Tl^{I}[(C_4H_9N_4)Pt^{II}(mnt)]$. There are a number of close contacts between the thallium ions and parts of neighboring platinum complexes. These interactions, which involve the cyano and sulfur donors on adjacent platinum complexes, provide a range of Coulombic forces which may serve to stretch the $Tl^{I}\cdots Pt^{II}$ bond.

Electronic Spectroscopy. The electronic absorption spectra of all of the compounds were measured in the solid state as KBr pellets. Although this technique tends to obscure all but the most gross features of the spectra, it is clear that the broad, low-energy band at 480 nm in the red polymorph of $Tl^{I}[(C_4H_9N_4)Pt^{II}(CN)_2]$ is unique within this group of compounds. In the solid state, the lowest-energy band of the

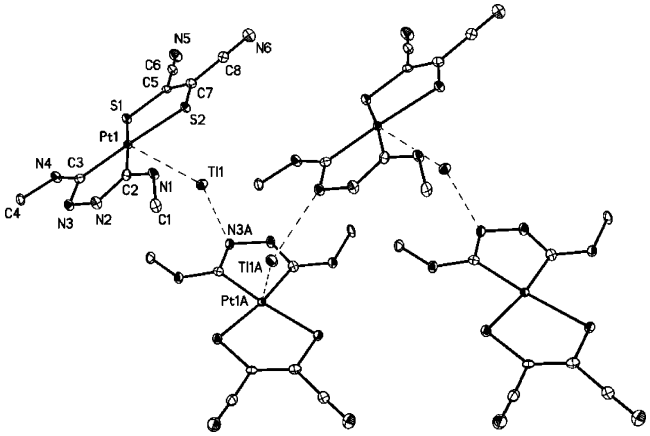

Figure 8. A drawing of a portion of the helical polymer chain in $Tl^{I}[(C_4H_9N_4)Pt^{II}(mnt)]$ with 50% thermal contours. The Tl1···Pt1 separation is 3.4400(2) Å, and the Pt1−Tl1−N3A angle is 102.59(6) °.

yellow polymorph of $Tl^{I}[(C_4H_9N_4)Pt^{II}(CN)_2]$ occurs at about 350 nm while $Tl^{I}[(C_4H_9N_4)Pt^{II}(mnt)]$ and $Tl^{I}[(C_4H_9N_4)Pt^{II}$-(dmg-H)]·$5H_2O$ have low-energy bands at about 415 and 430 nm, respectively.

The solution UV−visible spectroscopy of $Tl^{I}[(C_4H_9N_4)$-Pt^{II}(dmg-H)]·$5H_2O$ was studied in dimethylformamide (DMF) and dimethyl sulfoxide (DMSO), as well as in methanol. The spectrum of $Tl^{I}[(C_4H_9N_4)Pt^{II}$(dmg-H)]·$5H_2O$ in methanol, with a single low-energy feature at 420 nm, is virtually identical to that of $[(C_4H_9N_4)Pt^{II}$(dmg-H)]$^-$ in a solution prepared from $[(C_4H_{10}N_4)Pt^{II}$(dmg-H)] in methanol with a 0.10 M concentration of KOH. For comparison, a band occurs at about 415 nm in the solid-state UV−visible spectrum of $Tl^{I}[(C_4H_9N_4)Pt^{II}$(dmg-H)]·$5H_2O$. The band occurs at lower energy in DMF (434 nm) and DMSO (438 nm), displaying a negative solvatochromic effect in these more-polar solvents. Che has tentatively assigned this band, which occurs in all compounds involving the $(C_4H_9N_4)$-type ligands, as having Pt−π*(carbene) metal-to-ligand charge transfer (MLCT) character.[21] The low-energy bands we observe shows a good correlation in wavelength with Gutmann's solvent donor numbers[22] but no correlation with the corresponding acceptor number, a pattern which is consistent with the MLCT assignment with the solvent acting as a donor toward the metal. The solubility of $Tl^{I}[(C_4H_9N_4)$-Pt^{II}(mnt)] was too low in any solvent to obtain suitable spectra.

None of the $Tl^{I}-Pt^{II}$ complexes reported here are luminescent. However, $(C_4H_{10}N_4)Pt^{II}$(mnt)·H_2O does show luminescence as a solid and in dilute solution. The principle emission maximum occurs at 590 nm with an ~1400 cm^{-1} vibronic progression at higher energies (see Supporting Information). The excitation maximum occurs at 385 nm and overlaps with absorption maxima at 360 and 385 nm. Thus, there is a sizable Stokes' shift that suggests a distortion of the excited state. The luminescent behavior of $(C_4H_{10}N_4)$-Pt^{II}(mnt)·H_2O is similar to that of (1,5-cyclooctadiene)Pt^{II}-(mnt), which also shows an ~1400 cm^{-1} vibronic progression.[23] Consequently, the emission from $(C_4H_{10}N_4)Pt^{II}$(mnt)·H_2O is likely to arise from a MLCT process as noted previously for (1,5-cyclooctadiene)Pt^{II}(mnt).[22]

Discussion

There are now a number of complexes known that involve some sort of Tl···Pt interaction. Table 1 gives an overview of these along with the Tl···Pt distances in each. In this table, we have excluded $[Pt_2Tl_4(C{\equiv}CR)_8]$, which has thallium ions interacting with the ligands.[24] As seen in this table, a number of bonding motifs and oxidation states are found in complexes with some degree of Tl···Pt bonding.

Complexes with $Tl^{I}\cdots Pt^{II}$ interactions, which include the new complexes reported here, are particularly prevalent. Complexes in this class have $Tl^{I}\cdots Pt^{II}$ distances in the 2.79−3.44 Å range. The $Tl^{I}\cdots Pt^{II}$ interaction in $Tl^{I}[(C_4H_9N_4)Pt^{II}$-(mnt)] is at the far end of this range and is considerably longer than the next longest distance (3.140(1) Å) found in $Tl^{I}_2[Pt^{II}(CN)_4]$. Within the group of complexes with $Tl^{I}\cdots Pt^{II}$ interaction, the red polymorph of $Tl^{I}[(C_4H_9N_4)Pt^{II}$-$(CN)_2]$ is unique in that it is the only one with an extended chain structure that involves linear Pt···$(Tl\cdots Pt)_n$···Tl interactions. As noted earlier, the red color of this compound results from a transition at 480 nm in the visible absorption spectrum of the solid.[14] Such a feature is absent from the spectrum of the yellow polymorph and likely is due to the extended $Tl^{I}\cdots Pt^{II}$ interactions present in the red polymorph. Dimeric arrangements that produce simple pairs of $Tl^{I}\cdots Pt^{II}$ interactions are found in the yellow polymorph of Tl^{I}-$[(C_4H_9N_4)Pt^{II}(CN)_2]$ and in $Tl^{I}[(C_4H_9N_4)Pt^{II}$(dmg-H)]·$5H_2O$. $Tl^{I}[(C_4H_9N_4)Pt^{II}$(mnt)] also has simple $Tl^{I}\cdots Pt^{II}$ interactions in an extended helical arrangement, as seen in Figure 8. There are also examples of complexes with two Tl^{I} ions surrounding one pseudo-octahedrally coordinated Pt^{II} center, a situation exemplified by $Tl^{1}_2[Pt^{II}(CN)_4]$.[5] Additionally, there is one complex that has at Tl^{I} center surrounded by two planar Pt^{II} units.[25]

The bonding interactions between the metal centers in the s^2-d^8 ($Tl^{I}\cdots Pt^{II}$) complexes considered here result from a combination of metallophillic and Coulombic factors. For example, computations involving $Tl^{1}_2[Pt^{II}(CN)_4]$ have shown that the Pt···Tl bond consists of an ionic component which accounts for 87% of the bonding and a covalent, metallophillic interaction that accounts for the remaining 13% of the bond strength.[7] Additionally, theoretical studies have shown that interaction of the thallium ion with the adjacent nitrile groups of neighboring complexes in $Tl^{1}_2[Pt^{II}(CN)_4]$ diminishes the strength of the Pt···Tl bond.[26] Similarly, in $Tl^{I}[(C_4H_9N_4)Pt^{II}$(mnt)], the local coordination about the thallium ion, which is shown in the stereoview in Figure 9, may be the cause of the rather long Pt···Tl bond in this

(21) Lai, S. W.; Chan, M. C. W.; Wang, Y.; Lam, H. W.; Peng, S. M.; Che, C. M. *J. Organomet. Chem.* **2001**, *617*−*618*, 133.
(22) Gutmann, V. *Electrochim. Acta* **1976**, *21*, 670. (b) Marcus, Y. *J. Solution Chem.* **1984**, *13*, 599.
(23) Bevilacqua, J.; Zuleta, J. A.; Eisenberg; R. *Inorg. Chem.* **1993**, *32*, 3689.
(24) Berenguer, J. R.; Forniés, J.; Gomez, J.; Lalinde, E.; Merino, M. T. *Organometallics*, **2001**, *20*, 4847.
(25) Renn, O.; Lippert, B.; Mutikainen, I. *Inorg. Chim. Acta* **1993**, *208*, 219.
(26) Dolg, M.; Pyykkö, P.; Runeberg, N. *Inorg. Chem.* **1996**, *35*, 7450.

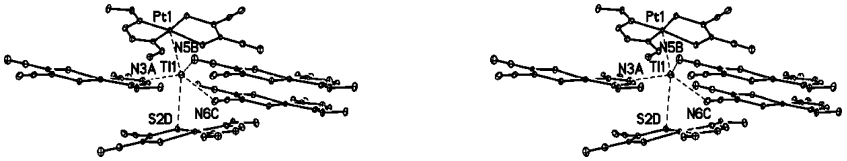

Figure 9. A stereoview of the thallium environment in $Tl^{I}[(C_4H_9N_4)Pt^{II}(mnt)]$ with 50% thermal contours. Selected distances (Å): Pt1−Tl1, 3.4400(2); N3A-Tl1, 2.708(3); N5B−Tl1, 3.027(3); N6C−Tl1, 3.241(3); S2D−Tl1, 3.3187(8).

Table 1. Tl···Pt Distances in Complexes

compound	Tl···Pt distance (Å)	arrangement	ref[a]
	$Tl^{I}\cdots Pt^{II}$		
$Tl^{I}[(C_4H_9N_4)Pt^{II}(CN)_2]$ (red polymorph)	3.0978(2)	$(Tl\cdots Pt)_n$	1
$Tl^{I}[(C_4H_9N_4)Pt^{II}(CN)_2]$ (yellow polymorph)	3.0256(5)	Tl···Pt	1
$Tl^{I}[(C_4H_9N_4)Pt^{II}(dmg\text{-}H)]\cdot 5H_2O$	3.0843(5)	Tl···Pt	this work
$Tl^{I}[(C_4H_9N_4)Pt^{II}(mnt)]$	3.4400(2)	Tl···Pt	this work
$Tl^{I}_2[Pt^{II}(CN)_4]$	3.140(1)	Tl···Pt···Tl (180°)	2
$[Tl^{I}(crown\text{-}P_2)Pt^{II}(CN)_2](NO_3)$	2.911(2)	Tl···Pt	3
$Pt^{II}Tl^{I}_2(C_6F_5)_2(C{\equiv}CPh)_2(acetone)_2]_2$	2.9921(5)	Tl···Pt···Tl (141.867(14)°)	4
	3.0274(6)		
$Tl^{I}_2Pt^{II}((C_6F_5)_2(C{\equiv}C\text{-}t\text{-}Bu)_2$	3.135(1)	Tl···Pt···Tl (180°)	5
$(\mu\text{-}MeCO_2)Tl^{I}Pt^{II}(C_6F_5)_2PPh_3$	2.994(1)	Tl···Pt	6
$[(\mu\text{-}MeCO_2)_2Tl^{I}_2Pt^{II}_2(C_6F_5)_6]^{2-}$	2.884(1)	Tl···Pt	6
$[(NH_3)_2Pt^{II}(1\text{-}Me\text{-}thyminato)_2\,Tl^{I}$	3.085(1)	Pt···Tl···Pt (136.7(1)°)	7
$(1\text{-}Me\text{-}thyminato)_2\,Pt^{II}(NH_3)_2](NO_3)$			
$Tl^{I}Pt^{II}CH_2Ph(Ph_2PCH_2\text{-}oxazolino)$	3.0942(9)	Tl···Pt	8
$Me_2Pt^{II}Tl^{I}\{\mu\text{-}Ph_2P)_2py\}Pt^{II}Me_2$	2.7961(7)	Pt···Tl···Pt (157.88(2)°)	9
	2.8090(7)		
	$Tl^{II}\cdots Pt^{II}$		
$(n\text{-}Bu_4N)[Tl^{II}Pt^{II}(C_6F_5)_4]$	2.708(1)	Pt···Tl···Pt (179(1)°)	10
	2.698(1)		
	$Tl^{I}\cdots Pt^{IV}$		
$Tl^{I}Pt^{IV}(CN)_5$	2.627(2)	Tl···Pt	11
$(dmso)_4Tl^{I}Pt^{IV}(CN)_5$	2.6131(4)	Tl···Pt	12
$(en)_2Tl^{I}Pt^{IV}(CN)_5$	2.6348(5)	Tl···Pt	12
$(bipy)(dmso)_3Tl^{I}Pt^{IV}(CN)_5$	2.6187(7)	Tl···Pt	13
$(bipy)_2Tl^{I}Pt^{IV}(CN)_5$	2.6117(5)	Tl···Pt	13
$(o\text{-}phen)(dmso)_3Tl^{I}Pt^{IV}(CN)_5$	2.6296(3)	Tl···Pt	14
$(o\text{-}phen)_2Tl^{I}Pt^{IV}(CN)_5$	2.6375(5)	Tl···Pt	14
	$Tl^{I}\cdots Pt^{0}$		
$[Tl^{I}Pt^{0}(PPh_2py)_3](NO_3)$	2.8888(5)	Tl···Pt	15
$[Tl^{I}Pt^{0}(PPh_2py)_3](CH_3CO_2)$	2.8653(4)	Tl···Pt	15
$[Tl^{I}Pt^{0}_2(P_2phen)_3]^{+}$	2.7907(9)	Pt···Tl···Pt (175.27(3)°)	16
$[Tl^{I}Pt^{0}_2(P_2bpy)_3]^{+}$	2.7953(2)	Pt···Tl···Pt (180°)	16
$[Tl^{I}Pt^{0}Au^{I}(P_2phen)_3]^{2+}$	2.7712(6)	Pt···Tl···Au (172.30(2)°)	17
	Cluster Complexes		
$[TlPt_3(CO)_3(PCy_3)_3]^{+}$	3.034(1), 3.047		18
$[Pt_3\{\mu_3Tl(diketonate)(OH_2)\}(\mu_3{-}CO)$	2.894(3), 2.891(3), 2.947(1)		19
$(\mu\text{-}dppm)_3][PF_6]_2$			

[a] 1. Stork, J. R.; Olmstead, M. M.; Balch, A. L. *J. Am. Chem. Soc.* **2005**, *127*, 6512. 2. Nagle, J. K.; Balch, A. L.; Olmstead, M. M. *J. Am. Chem. Soc.* **1988**, *110*, 319. 3. Balch, A. L.; Rowley, S. P. *J. Am. Chem. Soc.* **1990**, *112*, 6139. 4. Charmant, J. P. H.; Forniés, J.; Gómez, J.; Lalinde, E.; Merino, R. I.; Moreno, M. T.; Orpen, A. G. *Organometallics* **2003**, *22*, 652. 5. Ara, I.; Berenguer, J. R.; Forniés, J.; Gómez, J.; Lalinde, E.; Merino, R. I. *Inorg. Chem.* **1997**, *36*, 6461. 6. Usón, R.; Forniés, J.; Tomás, M.; Garde, R.; Merino, R. I. *Inorg. Chem.* **1997**, *36*, 1383. 7. Renn, O.; Lippert, B.; Mutikainen, I. *Inorg. Chim.* Acta, **1993**, *208*, 219. 8. Oberbeckmann-Winter, N.; Branstein, P.; Welter, R. *Organometallics* **2004**, *23*, 6311. 9. Song, H.-B.; Zhang, Z.-Z.; Hui, Z.; Che, C.-M.; Mak, T. C. W. *Inorg. Chem.* **2002**, *41*, 3146. 10. Usón, R.; Forniés, J.; Tomás, M.; Garde, R.; Alonso, P. J. *J. Am. Chem. Soc.* **1995**, *117*, 1837. 11. Jalilehvand, F.; Eriksson, L.; Glaser, J.; Maliarik, M.; Mink, J.; Sandström, M.; Tóth, I.; Tóth, J. *Chem. Eur.* J. **2001**, *7*, 2167. 12. Ma, G.; Kritikos, M.; Glaser, J. *Eur. J. Inorg. Chem.* **2001**, 1311. 13. Ma, G.; Kritikos, M.; Maliarik, M.; Glaser, J. *Inorg. Chem.* **2004**, *43*, 4328. 14. Ma, G.; Fischer, A.; Glaser, J. *Eur. J. Inorg. Chem.* **2002**, 1307. 15.Catalano, V. J.; Bennett, B. L.; Mutatidis, S.; Noll, B. C. *J. Am. Chem. Soc.* **2001**, *123*, 173. 16. Catalano, V. J.; Bennett, B. L.; Yson, R. L.; Noll, B. C. *J. Am.* Chem. Soc. **2000**, *122*, 10056. 17. Catalano, V. J.; Malwitz, M. A. *J. Am. Chem. Soc.* **2004**; *126*, 6560. 18. Ezomo, O. J.; Mingos, D. M. P.; Williams, I. D. *J. Chem. Soc., Chem. Commun.* **1987**, 924. 19. Stadnichenko, R.; Sterenberg, B. T.; Bradford, A. M.; Jennings, M. C.; Puddephatt, R. J. *J. Chem. Soc., Dalton Trans.* **2002**, 1212.

compound. The metallophillic interaction in these $Tl^{I}\cdots Pt^{II}$ complexes, including the ones reported here, results from σ bonding that involves the filled 6s and empty $6p_z$ orbitals on thallium and the filled d_{z^2} and empty p_z orbitals on platinum.[5,24] Since the metallophillic interaction between thallium and platinum contributes only a fraction to the bonding in these complexes, it is not unexpected that the length of the $Tl^{I}\cdots Pt^{II}$ bonds change as the ancillary ligands in these complexes are altered and as the patterns of hydrogen bonding within these solids vary.

For the complexes reported here, there are a number of weak interactions beyond the $Tl^{I}\cdots Pt^{II}$ bonds that contribute to the solid-state organization. In particular, for the red and yellow polymorphs of $Tl^{I}[(C_4H_9N_4)Pt^{II}(CN)_2]$ and $Tl^{I}[(C_4H_9N_4)Pt^{II}(dmg\text{-}H)]\cdot 5H_2O$, the planar complexes are arranged into layers, as seen in Figures 4 and 5. In these layers,

Table 2. Crystallographic Data

	$[(C_4H_{10}N_4)Pt(dmg\text{-}H)]\cdot 3H_2O$	$Tl^I[(C_4H_9N_4)Pt^II(dmg\text{-}H)]\cdot 5H_2O$	$(C_4H_{10}N_4)Pt^{II}(mnt)\cdot H_2O$	$Tl^I[(C_4H_9N_4)Pt^II(mnt)]$
color/habit	orange needle	orange needle	colorless/pink dichroic plate	yellow needle
formula	$C_8H_{22}N_6O_5Pt$	$C_{16}H_{50}N_{12}O_{14}Pt_2Tl_2$	$C_8H_{12}N_6OPtS_2$	$C_8H_9N_6PtS_2Tl$
fw	477.41	716.80	467.45	652.79
cryst syst	monoclinic	triclinic	monoclinic	orthorhombic
space group	$P2_1/c$	$P\bar{1}$	$C2/m$	$P2_12_12_1$
a, Å	21.3520(18)	6.8447(6)	11.2211(11)	8.7253(18)
b, Å	7.0531(6)	12.2150(10)	16.2198(16)	11.071(2)
c, Å	23.395(3)	12.3250(11)	6.8987(7)	13.609(3)
α, deg	90	116.4430(10)	90	90
β, deg	123.213(2)	91.020(2)	94.7950(10)	90
γ, deg	90	103.837(2)	90	90
V, Å^3	2947.7(5)	886.68(13)	1251.2(2)	1314.6(5)
Z	8	2	4	4
T, K	90(2)	90(2)	90(2)	90(2)
λ, Å	0.71073	0.71073	0.71073	0.71073
d, g/cm^3	2.152	2.685	2.482	3.298
μ, mm^{-1}	9.550	16.997	11.545	23.179
R1 (obsd data)	0.022	0.036	0.023	0.035
wR2 (all data,	0.051	0.082	0.047	0.083

[a] For data with $I > 2\sigma I$: $R1 = (\sum||F_o| - |F_c||)/(\sum|F_o|)$. [b] For all data: $wR2 = \sqrt{\sum[w(F_o^2-F_c^2)^2]/\sum[w(F_o^2)^2]}$.

there are interactions between the thallium atoms and the nitrogen atoms of the cyano ligands and hydrogen bonds between the inner N−H groups of the chelating carbene ligands and the nitrogen atoms of the cyanide ligands that facilitate close packing of the constituents. The thallium ion environments in these $Tl^I\cdots Pt^{II}$ compounds varies considerably, and that environment can influence the $Tl^I\cdots Pt^{II}$ distance. As noted above, Pyykkö and co-workers have argued that Coulombic interactions of the thallium ion in $Tl^1_2[Pt^{II}(CN)_4]$ with nitrogen atoms of nearby complexes serve to lengthen the $Tl^I\cdots Pt^{II}$ bond in the solid state. In $Tl^I[(C_4H_9N_4)Pt^{II}(dmg\text{-}H)]\cdot 5H_2O$ and in the red and yellow polymorphs of $Tl^I[(C_4H_9N_4)Pt^{II}(CN)_2]$, the thallium ion is coordinated by only two groups other than the $Tl^I\cdots Pt^{II}$ interaction. However, in $Tl^I[(C_4H_9N_4)Pt^{II}(mnt)]$ the thallium environment is more complex, as seen in Figure 9, and the added Coulombic interactions with the neighboring groups may be responsible for the long $Tl^I\cdots Pt^{II}$ distance in the compound.

Complexes involving a Tl^I-Pt^{IV} (or alternatively a $Tl^{II}-Pt^{III}$) interaction display shorter Tl−Pt distances than found in complexes with $Tl^I\cdots Pt^{II}$ interactions. Thus, the Tl−Pt distance in $Tl^IPt^{IV}(CN)_5$ is 2.627(2) Å, a distance indicative of the presence of a strong bond between the two metal centers. Computational studies on an $[H_5Pt-TlH]^-$ analogue suggest that the Tl−Pt bond is formed by σ-donation from thallium to platinum coupled with π-donation from the orthogonal Pt−H bonds to the 6p thallium orbitals to produce a Tl≡Pt bond.[27] Similarly, the Tl−Pt distances in paramagnetic $(n\text{-}Bu_4N)[Tl^{II}Pt^{II}(C_6F_5)_4]$ are also rather short: 2.708(1), 2.698(1) Å.[28]

With complexes that involve $Tl^I\cdots Pt^0$ interactions, the Tl−Pt distances fall in the range 2.77−2.89 Å. The ranges of distances in complexes with the s^2-d^8 ($Tl^I\cdots Pt^{II}$) and s^2-d^{10} ($Tl^I\cdots Pt^0$) electronic structures are similar. In part, this might be expected, since platinum uses filled d_{z^2} and empty p_z orbitals to interact with the filled s^2 and empty p_z orbitals on thallium in both cases. While Pt(0) is generally larger than Pt(II), Coulombic repulsion may also contribute to lengthening the Tl(I)−Pt(II) bonds.

It is interesting to note that neither $[(C_4H_{10}N_4)Pt^{II}(dmg\text{-}H)]\cdot 3H_2O$ nor $(C_4H_{10}N_4)Pt^{II}(mnt)\cdot H_2O$ undergo self-association in the solid state. In contrast, the cation, $[(C_4H_9N_4)Pt^{II}(CNCH_3)_2]^+$, crystallizes in a variety of self-associated structural motifs in which Pt···Pt interactions play a prominent role.[3] These structural motifs differ depending upon the anion used to form the salt and in some cases the degree of hydration of the crystals.

Experimental Section

Materials. The compounds $(C_4H_{10}N_4)Pt^{II}(CN)_2$, $(C_4H_{10}N_4)Pt^{II}(dmg\text{-}H)$, and $(C_4H_{10}N_4)Pt^{II}Cl_2$ were prepared according to established procedures.[22,27] The red and yellow polymorphs of $Tl[(C_4H_9N_4)Pt(CN)_2]$ were obtained as previously described.[15] Maleonitrile disodium salt (Na_2mnt) (Fluka Chemika) was recrystallized from absolute ethanol by addition of ethyl ether. All other reagents were commercially available and used without further purification. (***CAUTION:*** *Thallium compounds are highly toxic and should be handled with extreme care.*)

$Tl^I(C_4H_9N_4)Pt^{II}(dmg\text{-}H)\cdot 5H_2O$. A solution of 0.0754 g (0.2830 mmol) of thallium(I) nitrate in 1.5 mL of 0.10 M aqueous potassium hydroxide was added to a solution of 0.1097 g (0.280 mmol) of $(C_4H_{10}N_4)Pt^{II}(dmg\text{-}H)$ in 3.5 mL of 0.10 M aqueous potassium hydroxide. A brick red precipitate formed overnight. The somewhat soluble precipitate was carefully washed with water, ethanol, and ether and air-dried to yield 0.0680 g (0.114 mmol, 40.7%) of the product. Diffraction-quality crystals, which formed as thin orange needles, were prepared by adding a solution of 0.0028 g (0.010 mmol) of thallium(I) nitrate in 0.5 mL of 0.10 M potassium hydroxide to a solution of 0.0040 g (0.010 mmol) of $(C_4H_{10}N_4)Pt^{II}(dmg\text{-}H)$ in 0.5 mL of 0.10 M potassium hydroxide. Orange needles grew overnight. On heating, the compound loses water at 100−110 °C and decomposes at 210−212 °C. $Tl^I(C_4H_9N_4)Pt^{II}(dmg\text{-}H)\cdot 5H_2O$ is soluble in methanol, dimethyl sulfoxide, and dimethylformamide. ^1H NMR (300 MHz) in CD_3OD: δ 2.11 (s, 6H), 2.95 (s, 6H), N−H resonances are not observed due to exchange

(27) Pyykkö, P.; Patzschke, M. *Faraday Discuss.* **2003**, *124*, 41.
(28) Usón, R.; Forniés, J.; Tomás, M.; Garde, R.; Alonso, P. J. *J. Am. Chem. Soc.* **1995**, *117*, 1837.

with deuterated solvent. Infrared spectrum (cm^{-1}): 684 s, 968 w, 1047 m, 1207 m, 1376 m, 1464 w, 1532 s, 1585 w, 3042 br, 3156 br.

$(C_4H_{10}N_4)Pt^{II}(mnt)\cdot H_2O$. A 0.1561 g (0.411 mmol) portion of $(C_4H_{10}N_4)Pt^{II}Cl_2$ was dissolved in a minimal amount of ammonium hydroxide, and a solution of 0.1565 g (0.841 mmol) of Na_2mnt in 10 mL of ethanol was added. The mixture was gently warmed for 15 min and then cooled to 0 °C. Enough of a 6 M solution of hydrochloric acid was added to acidify the solution to a pH of 3 with stirring. The tan product precipitated. It was collected by filtration and washed successively with water, wet ethanol, absolute ethanol, and ether and then air-dried to yield an off-white powder that had a red luminescence when irradiated at 366 nm. The product was isolated in quantitative yield. Diffraction-quality crystals were prepared by recrystallization from boiling methanol to give colorless/pink dichroic plates that had a red luminescence. Upon heating, the solid loses water at ∼100 °C and decomposes at 259−261 °C. $(C_4H_{10}N_4)Pt^{II}(mnt)\cdot H_2O$ is soluble in dimethyl sulfoxide and dimethylformamide and slightly soluble in hot methanol. ^{1}H NMR (300 MHz) in dimethylformamide-d_7: δ 2.94 (d, J = 5 Hz, 6H) Me, 7.72 (br d, J = 5 Hz, 2H) N−H outer. Infrared spectrum (cm^{-1}): 890 w, 1003 w, 1025 w, 1051 w, 1091 w, 1108 w, 1142 m, 1151 m, 1208 m, 1246 w, 1292 w, 1365 m, 1454 m, 1474 s, 1497 m, 1526 s, 1601 s, 2191 m, 2203 m, 2215 w, 2304 vw, 2826 w, 2867 w, 2914 w, 2949 w, 3013 w, 3064 w, 3109 w, 3145 w, 3231 m br, 3408 m, 3481 m br.

$Tl^I[(C_4H_9N_4)Pt^{II}(mnt)]$. A 0.1512 g (0.3364 mmol) sample of $(C_4H_{10}N_4)Pt^{II}$(mnt) was dissolved in 15 mL of 0.1 M aqueous potassium hydroxide. A solution of 0.0944 g (0.354 mmol) of thallium(I) nitrate in 3 mL of 0.10 M aqueous potassium hydroxide was added. The yellow, microcrystalline precipitate that formed was collected by filtration and washed with 0.10 M potassium hydroxide, ethanol, and ether. After air-drying, 0.1067 g (0.1634 mmol, 48.6%) of an orange-tan powder was obtained. Diffraction-quality crystals were obtained by adding a solution of 0.0027 g (0.010 mmol) of thallium(I) nitrate in 0.5 mL of 0.1 M KOH to a solution of 0.0046 g (0.010 mmol) of $(C_4H_{10}N_4)Pt^{II}$(mnt) in 1.0 mL of 0.1 M KOH. Dark orange-yellow blocks grew within 3 days. The crystals decompose at 246−249 °C. $Tl^I[(C_4H_9N_4)Pt^{II}(mnt)]$ is very slightly soluble in water. Infrared spectrum (cm^{-1}): 869 w, 1015 m, 1050 m, 1110 w, 1149 m, 1179 w, 1264 m, 1362 m, 1398 w, 1467 s, 1505 s, 1575 m, 2201 m br, 3300 m br, 3398 m br.

Physical Measurements. Infrared spectra were recorded as neat powders on a Mattson Genesis II FT-IR spectrometer fitted with a Specac ATR accessory. Electronic absorption spectra were recorded using a Hewlett-Packard 8450A diode array spectrophotometer.

X-Ray Crystallography and Data Collection. The crystals were removed from the glass tubes in which they were grown together with a small amount of mother liquor and immediately coated with a hydrocarbon oil on the microscope slide. Suitable crystals were mounted on glass fibers with silicone grease and placed in the cold dinitrogen stream of a Bruker SMART CCD with graphite-monochromated Mo Kα radiation at 90(2) K. No decay was observed in 50 duplicate frames at the end of each data collection. Crystal data are given in Table 2. The structures were solved by direct methods and refined using all data (based on F^2) using the software of SHELXTL 5.1. A semiempirical method utilizing equivalents was employed to correct for absorption.[29] Hydrogen atoms were located in a difference map, added geometrically, and refined with a riding model.

Acknowledgment. We thank the Petroleum Research Fund (Grant No. 37056-AC) for support, the Tyco Foundation for a fellowship for J.R.S, and the reviewers for constructive comments. The Bruker SMART 1000 diffractometer was funded in part by NSF Instrumentation Grant No. CHE-9808259.

Supporting Information Available: Emission, excitation, and absorption spectra for $(C_4H_{10}N_4)Pt^{II}$(mnt) and X-ray crystallographic files in CIF format for $[(C_4H_{10}N_4)Pt^{II}(dmg\text{-}H)]\cdot 3H_2O$, $Tl^I(C_4H_9N_4)Pt^{II}(dmg\text{-}H)\cdot 5H_2O$, $(C_4H_{10}N_4)Pt^{II}$(mnt), and $Tl^I[(C_4H_9N_4)Pt^{II}(mnt)]$. This material is available free of charge via the Internet at http://pubs.acs.org.

IC051252+

(29) SADABS 2.10, Sheldrick, G. M. based on a method of Blessing, R. H. *Acta Crystallogr. Sect. A* **1995**, *51*, 33.